Supplementary Material for

Active Pd nanoclusters supported on nitrogen/amino co-functionalized carbon for highly efficient dehydrogenation of formic acid

Dan Liu,[#1] Cheng Zhou,[#2] Ge Wang,[2] Yong Li,[2] Zhimao Yang,[1] Chuncai Kong*[1] and Ben Liu*[3]

[1]Ministry of Education Key Laboratory for Non-equilibrium Synthesis and Modulation of Condensed Matter, Shaanxi Province Key Laboratory of Advanced Functional Materials and Mesoscopic Physics, School of Physics, Xi'an Jiaotong University, Xi'an 710049, China. Email: kongcc@xjtu.edu.cn

[2]Beijing Institute of Control Engineering, Beijing 100190, P.R. China.

[3]Key Laboratory of Green Chemistry and Technology of Ministry of Education, College of Chemistry, Sichuan University, Chengdu 610064, China. Email: ben.liu@scu.edu.cn

SUPPORTING FIGURES

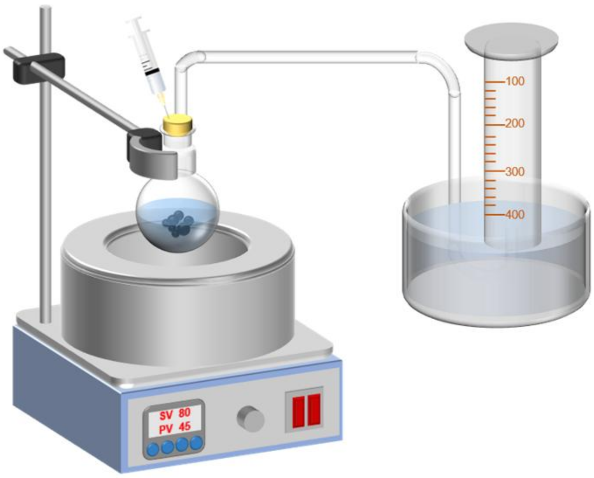

Supplementary Figure 1. Reaction set-up of formic acid dehydrogenation.

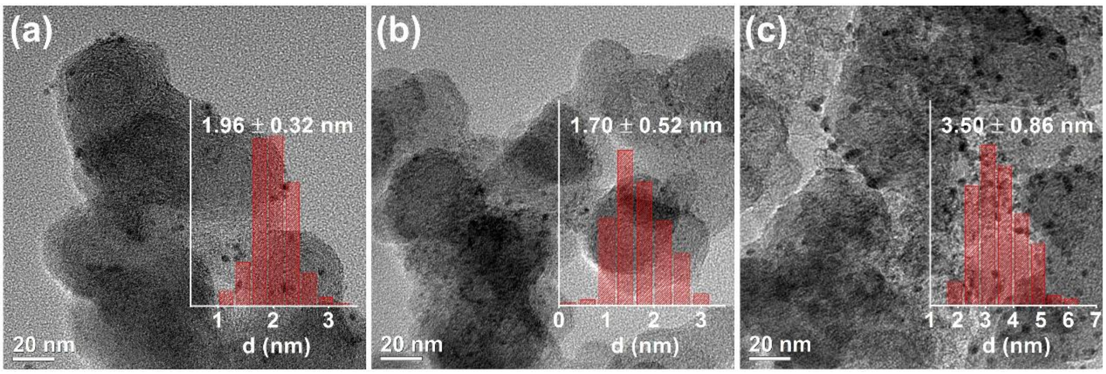

Supplementary Figure 2. TEM images of (a)Pd@NH_2-C, (b)Pd@NC, and (c) Pd@C.

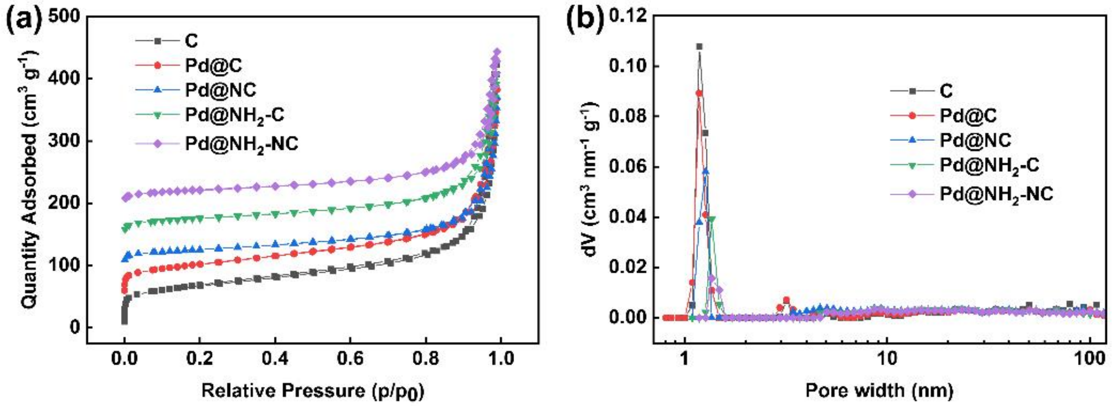

Supplementary Figure 3. (a) N_2 sorption isotherms and (b) corresponding pore-size distribution curves of C, Pd@C, Pd@NC, Pd@NH_2-C, and Pd@NH_2-NC.

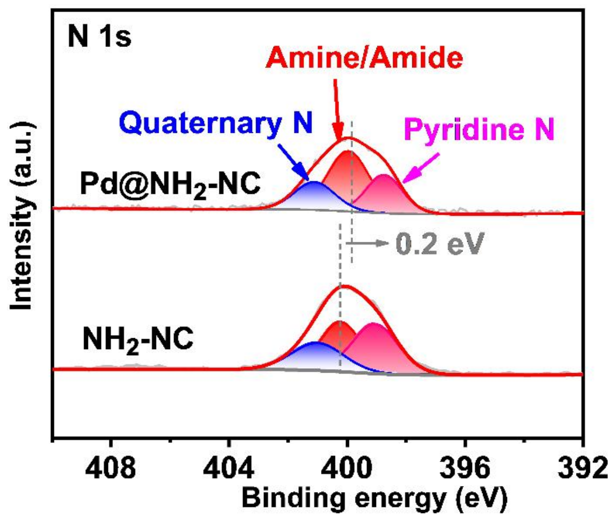

Supplementary Figure 4. High-resolution XPS spectra of N 1s for NH_2-NC and Pd@NH_2-NC.

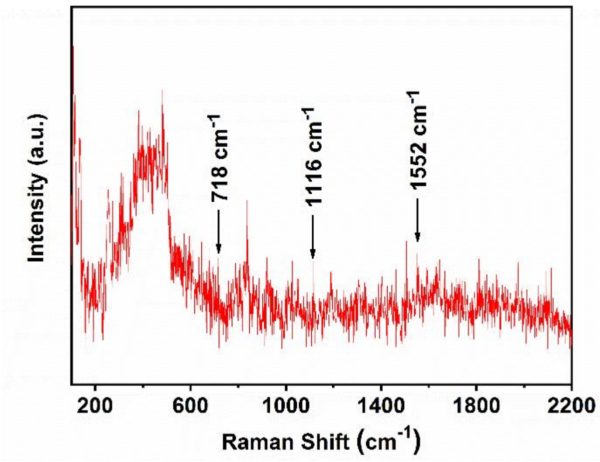

Supplementary Figure 5. Raman spectra of the reaction process of FA dehydrogenation with Pd@NH_2-NC catalyst in FA aqueous solution.

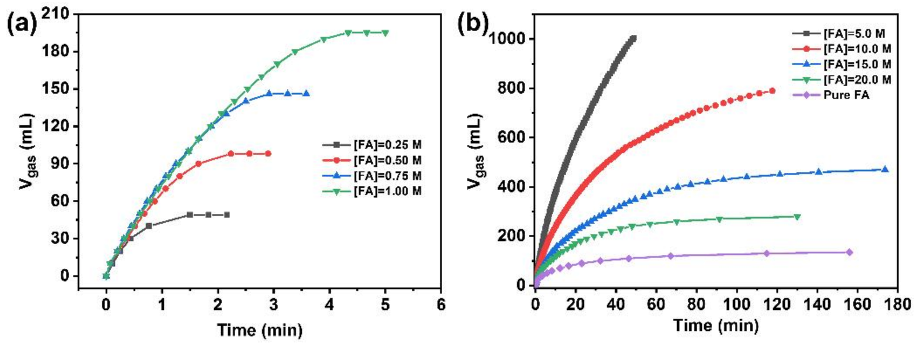

Supplementary Figure 6. Generated V(H_2 + CO_2) versus time for the dehydrogenation of FA at 298 K over Pd@NH_2-NC with different FA concentrations.

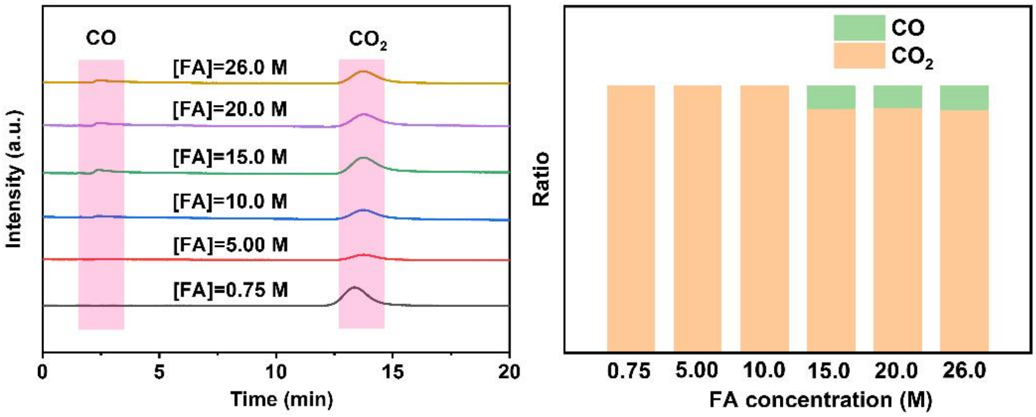

Supplementary Figure 7. Gas chromatography analysis results for gas generated from FA dehydrogenation with different FA concentrations.

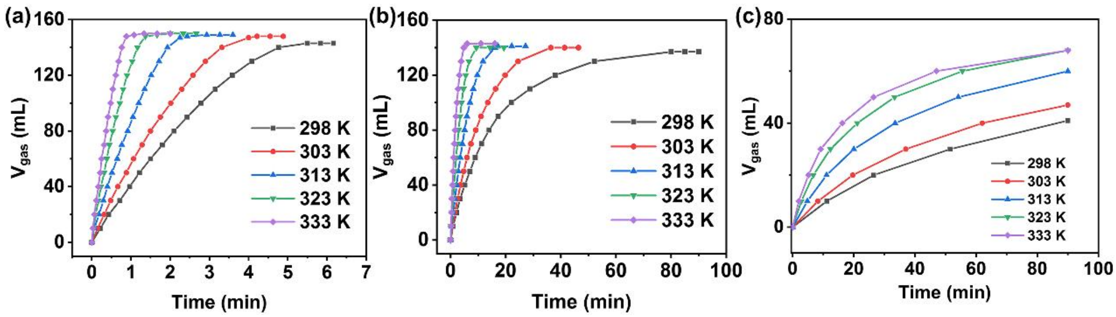

Supplementary Figure 8. (a-c) Generated V(H_2 + CO_2) versus time for the dehydrogenation of FA over (a) Pd@NH_2-C, (b) Pd@NC, and (c) Pd@C under different temperatures.

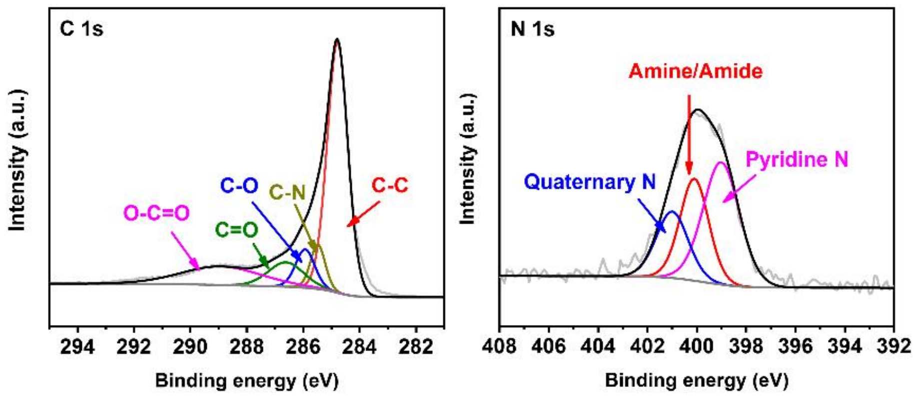

Supplementary Figure 9. (a) High-resolution XPS C 1s and (b) N 1s spectra of Pd@NH_2-NC after the stability tests for five cycles.

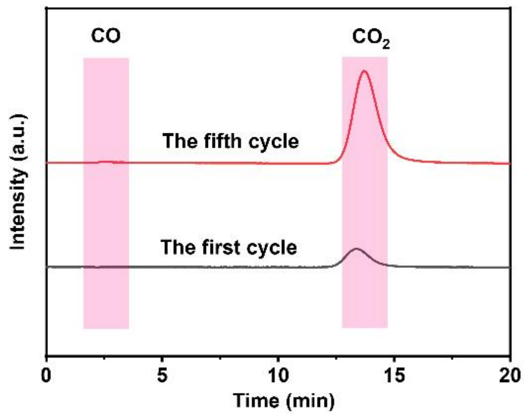

Supplementary Figure 10. Gas chromatography analysis for gas generated from FA dehydrogenation at the first and fifth cycles.

Supplementary Table S1. Comparison of key parameters of Pd@NH_2-NC for the FA dehydrogenation with other reported catalysts.

Catalysts	*Temp.* (K)	Additive	E_a (kJ mol^{-1})	*TOF* (h^{-1})	Ref.
Pd@NH_2-NC	333	None	28.5	15788[a]	This work
$Pd_{0.8}Au_{0.2}$/UiO-66-D	333	None	32.01	3122[a]	[1]
//$_{0.8}Pd_{0.2}Ni(OH)_2$@S-1	333	None	52.4	5803[a]	[2]
Pd-MnO_x/SiO_2-NH_2	333	None	61.9	2150[a]	[3]
Pd/NHPC-AC	333	HCOONa	21.5	4115[a]	[4]
Ag_2Pd_8/TiO_2-M-450	333	HCOONa	35.52	4789[a]	[5]
Arg-Pd/MSC-30	333	HCOONa	43.99	5723[c]	[16]
Pd@NH_2-NC	323	None	28.5	11947[a]	This work
$Cr_{0.4}Pd_{0.6}$/MIL-101-N H_2	323	None	43.5	2009[a]	[6]
$Pd_{0.8}Au_{0.2}$/UiO-66-(N $H_2)_2$	323	None	32.01	3660[a]	[7]
$Cr_{0.4}Pd_{0.6}$/M-β-CD-A	323	None	49.4	5771[a]	[8]
Pd/MSC-30	323	HCOONa	38.6	2623[a]	[9]
Pd–WO_x/(P)NPCC	323	HCOONa	35.9	6135[a]	[10]
Pd/CN_{ZM}	323	HCOONa	37.51	4157[d]	[17]
Pd@NH_2-NC	303	None	28.5	5609[a]	This work
Pd@$Bi_{0.11}$/C	303	HCOONa	44	4350[b]	[18]
Pd-N_{30}/C	303	HCOONa	-	3481	[19]
PdP/NC	303	HCOONa	27.2	3253[d]	[20]
Pd@NH_2-NC	298	None	28.5	4892[a]	This work
$Pd_{60}Au_{40}$/HPC-NH_2	298	None	30.6	3763[a]	[11]
$Ni_{0.4}Pd_{0.6}$/NH_2-N-rGO	298	None	-	954.3[a]	[12]
Au_1Pd_3/BNNFs-A	298	None	20.1	1181.1[a]	[13]
Pd_8Ag_1/NH_2-TNS-rG O	298	None	22.0	1090[a]	[14]
Pd/NHPC-NH_2	298	None	46.3	1265[a]	[15]
Pd/NH_2-TPC	298	None	24.6	4312a	[21]

[a]*TOF value based on the initial 20% conversion of FA*

[b]*TOF value based on the initial 25% conversion of FA*

[c]*TOF value based on the time of half-completion of gas generation in an hour*

[d]*TOF value based on the complete conversion of FA*

REFERENCES

[1] Ding R, Li D, Li Y, Yu J, Jia M, Xu J. Bimetallic PdAu nanoparticles in amine-containing metal–organic framework UiO-66 for catalytic dehydrogenation of formic acid. *ACS Appl Nano Mater* 2021;4:4632−4641. [DOI: 10.1021/acsanm.1c00266]

[2] Sun Q, Wang N, Bing Q, et al. Subnanometric hybrid Pd-M$(OH)_2$, M= Ni, Co, clusters in zeolites as highly efficient nanocatalysts for hydrogen generation. *Chem* 2017;3:477–493. [DOI: 10.1016/j.chempr.2017.07.001]

[3] Bulut A, Yurderi M, Karatas Y, et al. Pd-MnO_x nanoparticles dispersed on amine-grafted silica: Highly efficient nanocatalyst for hydrogen production from additive-free dehydrogenation of formic acid under mild conditions. *Appl Catal B* 2015;164:324–333. [DOI: 10.1016/j.apcatb.2014.09.041]

[4] Chen Y, Li X, Wei Z, et al. Efficient synthesis of ultrafine Pd nanoparticles on an activated N-doping carbon for the decomposition of formic acid. *Catal Commun* 2018;108:55–58. [DOI: 10.1016/j.catcom.2018.01.028]

[5] Sun X, Li F, Wang Z, An H, Xue W, Wang Y. AgPd nanoparticles anchored on TiO_2 derived from a titanium metal–organic framework for efficient dehydrogenation of formic acid. *ChemCatChem* 2022;14:e202101528. [DOI: 10.1002/cctc.202101528]

[6] Gao D, Wang Z, Wang C, et al. CrPd nanoparticles on NH_2-functionalized metal-organic framework as a synergistic catalyst for efficient hydrogen evolution from formic acid. *Chem Eng J* 2019;361:953–959. [DOI: 10.1016/j.cej.2018.12.158]

[7] Ding R-D, Li Y-L, Leng F, et al. PdAu nanoparticles supported by diamine-Containing UiO-66 for formic acid dehydrogenation. *ACS Appl Nano Mater* 2021;4:9790−9798. [DOI: 10.1021/acsanm.1c02204]

[8] Wang H, Yue C, Gao D, et al. Enhancing formic acid dehydrogenation for hydrogen production with the metal/organic interface. *Appl Catal B* 2019;255:117776. [DOI: 10.1016/j.apcatb.2019.117776]

[9] Zhu Q-L, Tsumori N, Xu Q. Sodium hydroxide-assisted growth of uniform Pd nanoparticles on nanoporous carbon MSC-30 for efficient and complete dehydrogenation of formic acid under ambient conditions. *Chem Sci* 2014;5:195−199. [DOI: 10.1039/c3sc52448e]

[10] Zhang A, Xia J, Yao Q, Lu Z-H. Pd–WO_x heterostructures immobilized by

MOFs-derived carbon cage for formic acid dehydrogenation. *Appl Catal B* 2022;309:121278. [DOI: 10.1016/j.apcatb.2022.121278]

[11] Wang Z, Liang S, Meng X, Mao S, Lian X, Wang Y. Ultrasmall PdAu alloy nanoparticles anchored on amine-functionalized hierarchically porous carbon as additive-free catalysts for highly efficient dehydrogenation of formic acid. *Appl Catal B* 2021;291:120140. [DOI: 10.1016/j.apcatb.2021.120140]

[12] Yan J-M, Li S-J, Yi S-S, Wulan B-R, Zheng W-T, Jiang Q. Anchoring and upgrading ultrafine NiPd on room−temperature−synthesized bifunctional NH_2−N−rGO toward low−cost and highly efficient catalysts for selective formic acid dehydrogenation. *Adv Mater* 2018;30:1703038. [DOI: 10.1002/adma.201703038]

[13] Guo B, Li Q, Lin J, et al. Bimetallic AuPd nanoparticles loaded on amine-functionalized porous boron nitride nanofibers for catalytic dehydrogenation of formic acid. *ACS Appl Nano Mater* 2021;4:1849−1857. [DOI: 10.1021/acsanm.0c03224]

[14] Zhao X, Dai P, Xu D, Tao X, Liu X, Ge Q. Ultrafine PdAg alloy nanoparticles anchored on NH_2-functionalized 2D/2D TiO_2 nanosheet/rGO composite as efficient and reusable catalyst for hydrogen release from additive-free formic acid at room temperature. *J Energy Chem* 2021;59:455–464. [DOI: 10.1016/j.jechem.2020.11.018]

[15] Wang Z, Wang C, Mao S, Gong Y, Chen Y, Wang Y. Pd nanoparticles anchored on amino-functionalized hierarchically porous carbon for efficient dehydrogenation of formic acid under ambient conditions. *J Mater Chem A* 2019;7:25791–25795. [DOI: 10.1039/c9ta10196a]

[16] Hong C-B, Zhu D-J, Ma D-D, Wu X-T, Zhu Q-L. An effective amino acid-assisted growth of ultrafine palladium nanocatalysts toward superior synergistic catalysis for hydrogen generation from formic acid. *Inorg Chem Front* 2019;6;975. [DOI: 10.1039/c9qi00037b]

[17] Deng M, Yang A, Ma J, et al. Enhanced catalytic performance of N‑doped carbon sphere-supported Pd nanoparticles by secondary nitrogen source regulation for formic acid dehydrogenation. *ACS Appl Mater Interfaces* 2022;14;18550−18560. [DOI: 10.1021/acsami.2c02055]

[18] Qin X, Li H, Xie S, et al. Mechanistic analysis-guided Pd-based catalysts for

efficient hydrogen production from formic acid dehydrogenation. *ACS Catal* 2020;10;3921−3932. [DOI: 10.1021/acscatal.0c00225]

[19] Yu Y, Wang X, Liu C, Vladimir F, Ge J, Xing W. Surface interaction between Pd and nitrogen derived from hyperbranched polyamide towards highly effective formic acid dehydrogenation. *J Energy Chem* 2020;40;212-216. [DOI: 10.1016/j.jechem.2019.04.017]

[20] Zhu L, Liang Y, Sun L, Wang J, Xu D. Highly efficient dehydrogenation of formic acid over binary palladium−phosphorous alloy nanoclusters on N‑doped carbon. *Inorg Chem* 2021;60;10707-10714. [DOI: 10.1021/acs.inorgchem.1c01403]

[21] Shao X, Miao X, Tian F, et al. Amine-functionalized hierarchically porous carbon supported Pd nanocatalysts for highly efficient H2 generation from formic acid with fast-diffusion channels. *J Energy Chem* 2023;76;249-258. [DOI: 10.1016/j.jechem.2022.10.002]